Chapter 2

Influence of Alkali Metal Ions on Luminescence Behaviour of $Ca_{0.5}R_{1-x}(MoO_4)_2$:xLn^{3+} (R = Y, La), (Ln = Eu, Tb, Dy) Pulsed Laser Deposited Thin Phosphor Films

Jagannathan Thirumalai,
Venkatakrishnan Mahalingam and
Rajagopalan Krishnan

Additional information is available at the end of the chapter

http://dx.doi.org/10.5772/65006

Abstract

Thin phosphor films of $Ca_{0.5}R_{1-x}(MoO_4)_2$:xLn^{3+}, M^+ (R^{3+} = La, Y), (Ln^{3+} = Eu, Tb, Dy) (M^+ = Li^+, K^+ and Na^+) were deposited on quartz substrates by pulsed laser deposition (PLD) technique by ablation of a stoichiometric monocrystal target. The deposition was carried out using an Nd-YAG laser (λ = 1064 nm) in an ultra-high vacuum (UHV) with an oxygen back pressure of 300 mTorr at 600°C substrate temperatures. The laser-ablated films are optically active, as verified by the photoluminescence (PL) spectra, and the films exhibit smooth Stark levels. The photoluminescence of the $Ca_{0.5}R_{1-x}(MoO_4)_2$:xLn^{3+}, M^+ phosphors properties reveals characteristic visible emissions. Further, the co-doping of alkali metal chlorides MCl (M = Na, K, Li) into the $Ca_{0.5}R_{1-x}(MoO_4)_2$:xLn^{3+}, M^+ phosphor greatly improves the luminescence intensity, which can be explained by charge compensation effect. The fluorescence lifetime and photometric coordinates are discussed in detail.

Keywords: rare-earth and alkaline activated, thin phosphor films, pulsed laser deposition, surface morphology, luminescence

1. Introduction

The growth of good quality larger area thin film with homogeneous size distribution and morphology is still a demanding issue, and it is of significant attention towards the research fraternity. Remarkably, uniform micro/nano-structures have been paying global attention due to its potential application in high-performance luminescence and opto-electronic device based

on community their novel optical and electronic properties. To synthesize novel thin film materials such as molybdates [1, 2], tungstates [3], vanadates [4], and fluorides [5], copious prominent techniques are extensively adopted, for example chemical bath deposition (CBD), successive immersion layer adsorption reaction (SILAR), polymerization, electrodeposition, sputtering, metal-organic chemical vapour deposition (MO-CVD), molecular beam epitaxy (MBE), atomic layer deposition (ALD), pulsed laser deposition (PLD). In the midst of all, PLD is a multitalented method to prepare multiconstituent thin film materials in which raster examining of high-energy pulsed laser ablates the target material and produces the plasma plume [6, 7]. In recent times, the PLD technique has created a widespread usage with an exceptionally astonishing result in materials preparation and fabrication of a device in the opto-electronics field. Albeit the fabrication of optical quality of the thin films and waveguides using PLD technique with various technical hitches and burning issues, till date, these issues have undeniably been lucratively conquered, and quite a few good-quality thin films were grown by PLD.

1.1. Recent research scenario

In contrast to conventional incandescent and fluorescent lamps, white light emitting diode (w-LEDs) is seemed to be an optimistic solid-state light source with a good-quality energy conversion luminescence device [8]. By coalesce into the GaN blue LED chip with yellow emitting phosphor YAG:Ce^{3+} which yield a white light emission using the conventional technique [9–11]. Nevertheless, the deficient of red emission cog ends with low colour rendering index (CRI) and luminous efficacy of radiation (LER) which restricts their pertinence towards a few ambits [9, 12]. To conquer this hindrance, red or orange-red emitting ion such as Pr^{3+}, Sm^{3+}, Cr^{3+} and Mn^{2+} is co-doped with YAG:Ce^{3+} [10]. The other one is combining YAG:Ce^{3+} with red or orange-red phosphors such as nitrides (M_2SiN_8:Eu^{2+}), sulphides (CaS:Eu^{2+}), oxynitrides ($MSi_2O_2N_2$:Eu^{2+}) (where M = Ca, Sr) [10]. Furthermore, the enhancement of intense emission in the host material can be engendered by co-doping of alkali metal-chloride results in strong emission, which may possibly be an opportune and a generally suitable approach to acquire the phosphors with sufficient intensity and excellent efficiency are a great essential deal for prospective solid-state lighting devices [2]. Therefore, it is necessary to discover a suitable phosphor material with a sufficient chemical permanence with enhanced efficiency. Rare earth-doped phosphor materials are paying attention towards the research problems based on its applications in all the prospects of science and technology. Molybdates and tungstates with metallic elements form an essential class of phosphor materials. They belong to the scheelite family having a space group $I_{41/a}$. In both molybdate and tungstate family, the alkaline earth-based rare-earth-activated double molybdates are very much highly significant efficient materials on the basis of its unique structural, optical properties have come across profound applications in technological aspects. Alkaline rare-earth-activated tungstates having a general formula ARE $(MoO_4)_2$ (RE = Y, La; A = Ba, Ca, Sr) are considered as better luminescent hosts investigated significantly for various purposes such as photocatalysts [11], displays [8] and acquire substantial hydrolytic and thermal permanence. Furthermore, the electroluminescent devices in the form of thin films from these micro/nano-architectures are to be built for the white light emitting diode applications. Among the

http://dx.doi.org/10.5772/65006

aforesaid variety of fabrication of thin film techniques, pulsed laser deposition (PLD) is a viable method [2, 13, 14]. Nowadays, to fabricate homogeneous and large-scale thin films, laser rastering system attached into PLD technique has been used [13]. To consider the aspects of application, aforesaid reasons could make the PLD technique most unique and almost suitable for the growth and fabrication of good-quality micro/nano-thin films. It is interesting that the structural, optical, and photophysical properties of the micro/nano-architectures could be compared with the thin film phosphors and its bulk [2, 15] counter-parts.

In this viewpoint, we have prepared the single crystalline nano-thin phosphor films of $Ca_{0.5}R_{1-x}(MoO_4)_2:xLn^{3+}$ (R^{3+} = Y, La), (Ln^{3+} = Eu, Tb, Dy) with co-doping of alkali metal chlorides (0.02 M of LiCl, KCl, NaCl) have been ablated on quartz substrates using the pulsed laser deposition method (PLD). For the first time, the luminescence properties of these alkali chloride-activated phosphors are studied. The as-prepared molybdate and tungstate powders were further deposited as thin films using the laser-ablation by forming a ceramic target under oxygen atmosphere. Followed by the as-prepared samples was analyzed using X-ray diffraction (XRD), atomic force microscopy (AFM), field emission scanning electron microscopy (FESEM), photoluminescence (PL) spectroscopy, photometric characteristics using commission internationale de i'eclairage (CIE) diagrams. The colour chromaticity coordinates and luminescence decay times have also been determined and discussed in reference to the effect of alkali metal ions.

2. Experimental details

By employing the PLD technique, for the first time, the nano-thin phosphor films of $Ca_{0.5}R_{1-x}(MoO_4)_2:xLn^{3+}$ (x = 0.16 M) (R^{3+} = Y, La), (Ln^{3+} = Eu, Tb, Dy) with co-doping of alkali metal chlorides (0.02 M of LiCl, KCl, NaCl) were effectively coated on the quartz substrates by maintaining the substrate temperature of 600°C under oxygen atmospheric pressure (~300 mTorr). **Figure 1a–i** shows the images of different experimental procedures engaged for the growth of thin films.

2.1. Preparation of ceramic target, cleaning of substrates and growth of $Ca_{0.5}R_{1-x}(MoO_4)_2:xLn^{3+}$ nano-thin phosphor films

To prepare a strong and extremely impenetrable ceramic (molybdate and tungstate) target for laser ablation, the starting precursors such as Na_2CO_3, La_2O_3, Y_2O_3, MoO_3 and Ln_2O_3 (Ln = Eu, Tb, Dy) were taken in stoichiometric ratios along with 0.02 M of alkali chlorides (LiCl, KCl and NaCl), followed by using the agate mortar pestle the powders were grounded for 2 h. The doping concentrations of Ln^{3+} were optimized in our previous work [15] and kept at constant (0.16 M) for all the Ln^{3+} ions. Without using any binders, the homogeneously mixed powders were pressed and pelletized in the form of disk (pellet) at a pressure of 6 tons. By eliminating the unstable contaminants, shun pores, crack, and endorse densification, to promote the diffusion in atomic level all through the preparation of target [16]. Furthermore, the as-prepared pellet was annealed at 900°C for 3 h to achieve a very strong, stable and thick pellet

having a diameter of about 2.5 cm, and thickness of about 0.4 cm is attained. Then, the annealed target is used for laser ablation.

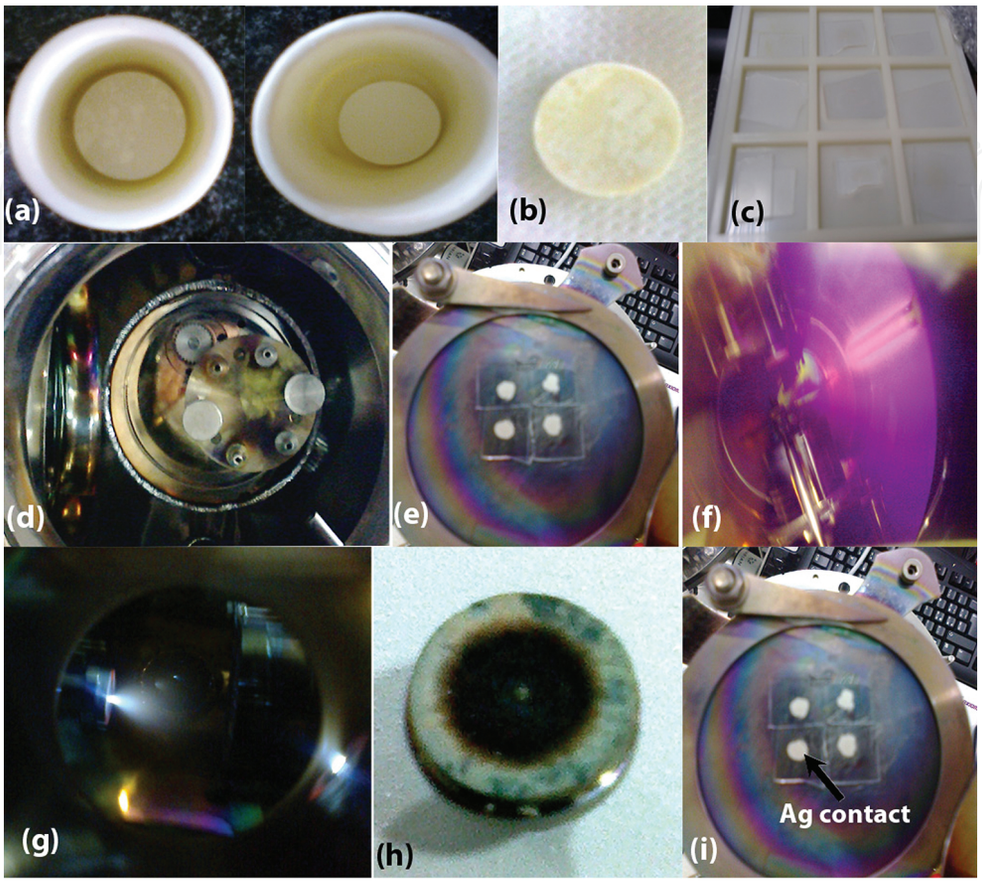

Figure 1. Photograph of different experimental methods demonstrating (a) homogeneously pelletized ceramic target, (b) high-temperature annealed target, (c) cleaning of substrates, (d) target loading, (e) loading of substrates, (f) impurities removal in UHV chamber (glow discharge), (g) laser ablation, (h) target after ablation, (i) thin films after deposition.

The procedure for predeposition cleaning of substrates and growth of nano-thin phosphor films were already discussed in detail on our previous work [2].

2.2. Characterization

The morphology of the product was analysed by field emission scanning electron microscope (FESEM-SUPRA 55). Using atomic force microscopy (NTEGRA PRIMA-NTMDT, USA), the surface topography of the thin phosphor films was studied. The crystal structure and phase purity of as-synthesized phosphor were recognized and confirmed by PANalytical's X'Pert PRO Materials Research X-ray Diffractometer (Almelo, USA) equipped with a CuKα radiation (λ = 0.154060 Å) at a scanning rate of 0.02°s^{-1} in a 2θ range of 15°–60°. Further, down-conversion PL excitation and emission studies and fluorescence decay time measurements were performed at room temperature using a Cary bench-top spectrophotometer (AGILENT Instruments, USA).

http://dx.doi.org/10.5772/65006

3. Results and discussion

3.1. Morphological and X-ray diffraction analysis

Figure 2a and **b** shows the scanning electron microscopy (SEM) images of $Ca_{0.5}R_{1-x}(MoO_4)_2$:xLn^{3+} (R^{3+} = Y, La), (Ln^{3+} = Eu, Tb, Dy) thin phosphor film co-doped with Li^+, K^+ and Na^+ metal ions prepared at 600°C with 300 mTorr. The as-prepared phosphor film comprises homogeneous nearly circular grains with a typical grain size around 250 nm. Based on the AFM studies, the surface topography, line profile and roughness of the prepared thin film was estimated. **Figures 3a** and **4a** show the 3D AFM image of thin film of $Ca_{0.5}R(MoO_4)_2$:Eu^{3+} (R = Y, La), and the scan was performed on 3 × 3 and 5 × 5 μm² area, respectively. From the 3D topographic image, the as-prepared thin phosphor film comprises of polished surface with uniform arrangement of the particles and with less agglomeration. The average roughness along with root-mean-square (rms) of the as-grown thin film was determined as 24.72 and 26.84 nm for $Ca_{0.5}R_{1-x}(MoO_4)_2$:xEu^{3+} (R^{3+} = Y, La). The 3D surface topography, 2D surface scan image, line profile, and histogram analysis are shown in **Figures 3a–d** and **4a–d**, respectively. Based on the scaling process, the particle size would be reduced to nano-scale in thin film which could be efficiently used for display applications. The optimization of maintaining different substrate temperature on rare-earth doped phosphors has been well examined and reported in our earlier work [2].

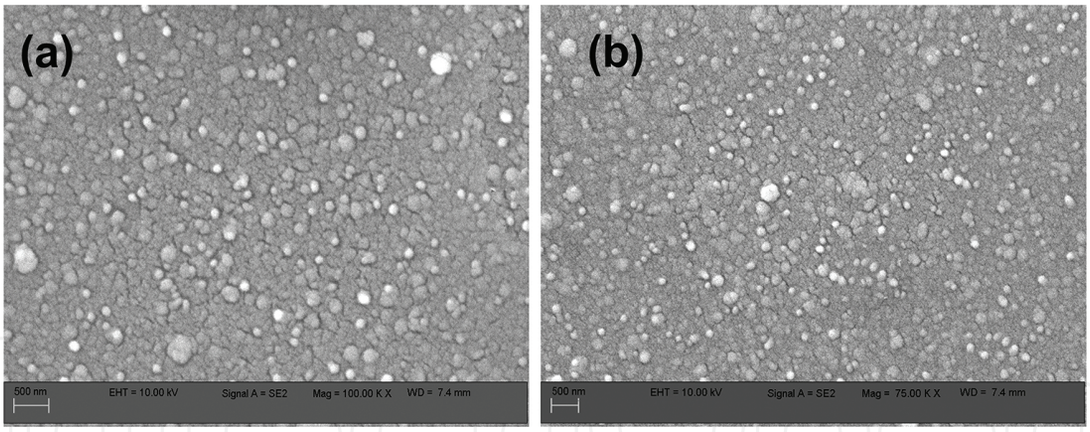

Figure 2. The SEM image (a and b) of $Ca_{0.5}R_{0.5}(MoO_4)_2$:Eu^{3+} (R^{3+} = Y, La) thin film.

The crystallinity and phase purity of the prepared products were examined using indexed powder X-ray diffraction patterns **Figure 5(a** and **b)** for as grown thin film samples. The compound $Ca_{0.5}Y_{(1-x)}(MoO_4)_2$:$xRE^{3+}$ crystallizes in the scheelite tetragonal crystal structure with a space group of $I_{41/a}$. The unit cell of $Ca_{0.5}Y_{(1-x)}(MoO_4)^2$ consists of $[MoO_4]^{2-}$ anions and Ca^{2+} and Y^{3+}/La^{3+} cations. In this phase, Mo sites are occupied by the molybdenum atoms (Mo^{6+}) and located at the centres of tetrahedron and surrounded by four equivalent oxygen (O^{2-}) atoms. The divalent Ca^{2+} and trivalent Y^{3+}/La^{3+} occupies the dodecahedral sites associated with the tetrahedral symmetry. The degree of dodecahedral and tetrahedral distortions is discussed in the previous work [2, 15, 17].

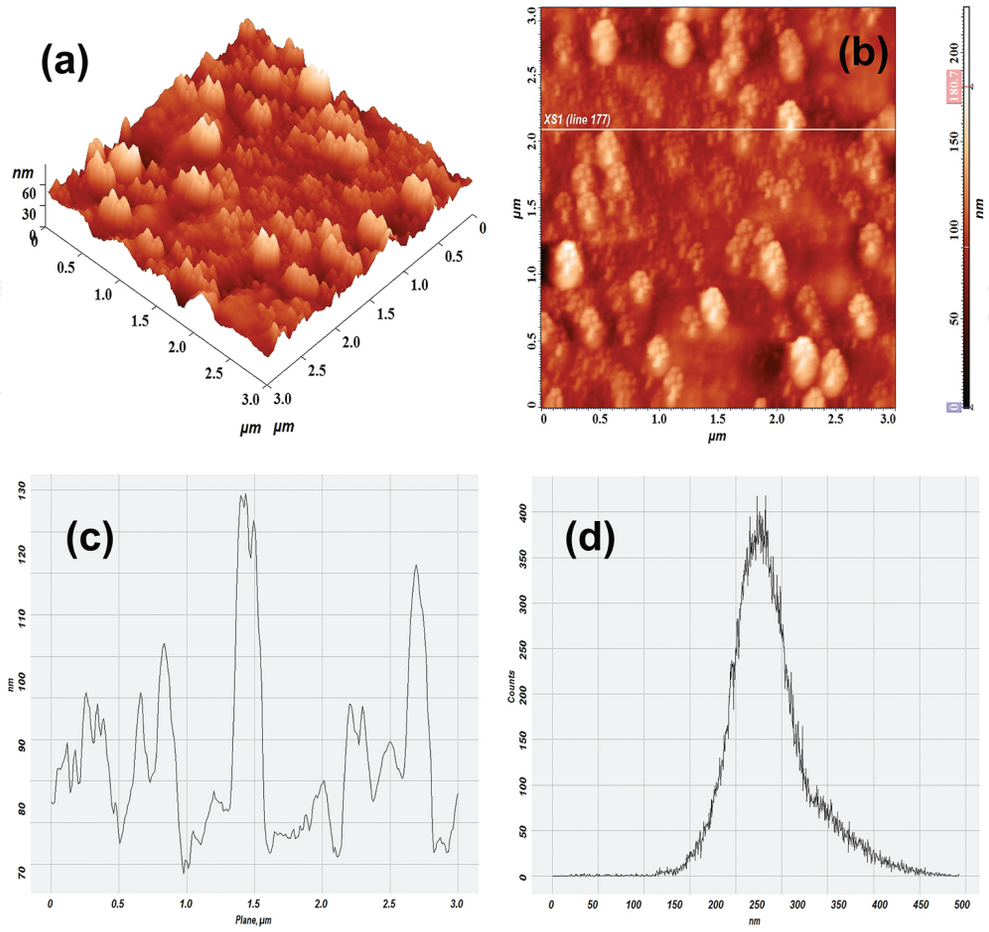

Figure 3. The AFM images of $Ca_{0.5}Y(MoO_4)_2:Eu^{3+}$ thin film (a) 3D surface topography, (b) 2D surface scan image, (c) line profile for vertical cross-section in 3 × 3 μm² scan area and (d) histogram analysis.

In the powder XRD pattern, all the peaks are indexed perfectly which indicates a pure tetragonal phase having scheelite crystal structure and the planes (1 0 1), (1 1 2), (0 0 4), (2 0 0), (2 0 4), (2 2 0), (1 1 6) and (1 3 2) are in well accordance with the JCPDS card no. 82-2369 of $NaY(MoO_4)_2$. No deleterious phases are found. The peak shift is not noticed with respect to doping. An intense peak with plane (1 1 2) is found at 28.95° [2, 15, 17].

3.2. Photoluminescence properties of laser-ablated thin phosphor films: $Ca_{0.5}R_{1-x}(MoO_4)_2:xLn^{3+},M^+$ (R = Y, La; Ln = Eu, Tb and Dy; M = Li, K and Na)

3.2.1. Enhancement of luminescence intensity by the persuade of alkali metal ions in $Ca_{0.5}R_{1-x}(MoO_4)_2:xLn^{3+},M^+$

In the phosphor material, by introducing the alkali metal chlorides, nitrates or fluorides, which substantially increase the luminescence intensity owing to the charge compensation effect between unequal ions [18]. On our previous work in $Ca_{0.5}R_{1-x}(MoO_4)_2:xLn^{3+}$ (R = Y, La) phosphor, the doping of alkali ions appreciably improves the emission properties by charge compensation using solid-state reaction method [15, 19].

http://dx.doi.org/10.5772/65006

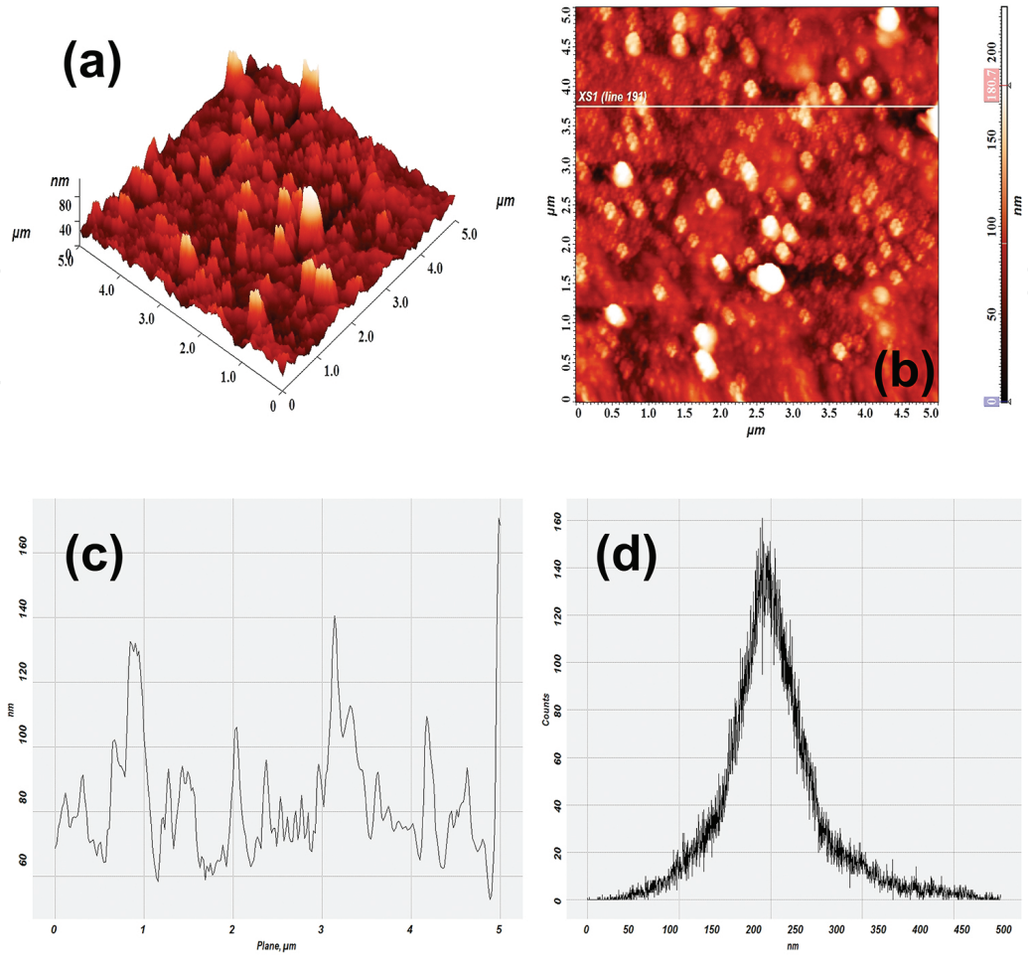

Figure 4. The AFM images of $Ca_{0.5}La(MoO_4)^2:Eu^{3+}$ thin film (a) 3D surface topography, (b) 2D surface scan image, (c) line profile for vertical cross-section in 5 × 5 μm² scan area and (d) histogram analysis.

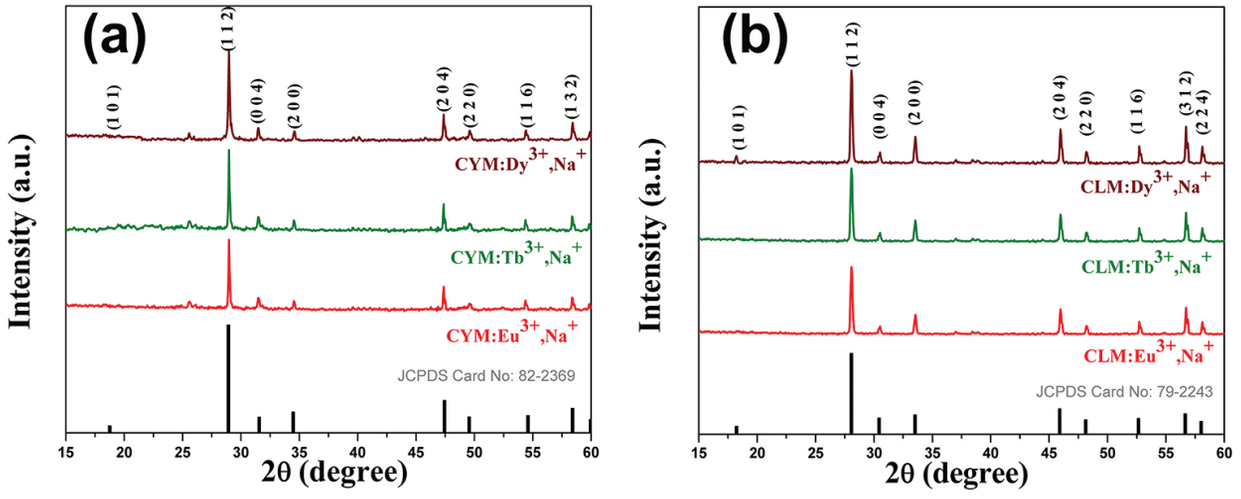

Figure 5. XRD patterns of (a) $Ca_{0.5}Y(MoO_4)_2:Ln^{3+},Na^+$, (b) $Ca_{0.5}La(MoO_4)_2:Ln^{3+},Na^+$ (Ln = Eu, Tb and Dy).

In our system, Eu^{3+}, Tb^{3+}, Dy^{3+} and M^{+} co-doped in $Ca_{0.5}R(MoO_4)_2$ (R = Y, La) matrix would induce a distortion in lattice, and consequently, the lattice symmetry is desperately lowered [20]. The co-doped Eu^{3+}, Tb^{3+}, Dy^{3+} and M^{+} at the Ca^{2+} sites in prepared thin film samples would play a role of dominance with enhanced luminescence intensity [21]. This is due to altering the symmetry and their surroundings in the locality of rare earth ions by adding the charge compensators of alkali metal ions [22]. **Figures 6** and **7** show the PL emission spectra of $Ca_{0.5}Y_{1-x}(MoO_4)_2{:}xLn^{3+},M^{+}$ (Ln = Eu, Tb and Dy; M = Li, K and Na) and $Ca_{0.5}La_{1-x}(MoO_4)_2{:}xLn^{3+}$, M^{+} (Ln = Eu, Tb and Dy; M = Li, K and Na) thin film phosphors. The luminescence emission intensity is deliberately increased for Na^{+} ion co-doped $Ca_{0.5}R_{1-x}(MoO_4)_2{:}xLn^{3+}$ (R = Y, La; Ln = Eu, Tb and Dy). This could be owing to the charge compensation effect, and the proposed mechanism is $Ca^{2+} \rightarrow 2M^{+}$ ($M = Li^{+}, K^{+}, Na^{+}$) [21, 22]. Furthermore, the ionic radius of Na^{+} (0.97 Å) is closer to the Ca^{2+} (1.12 Å) which is somewhat better than that of K^{+} (1.33 Å) and Li^{+} (0.59 Å) [3, 15]. Hence, there is an efficient replacement of Ca^{2+} ions by alkali metal ions. This forms the basis for the increased luminescence intensity, and obviously, Na^{+} is having the best charge compensation effect. The electronic configurations and its transitions are explained in the subsequent sections.

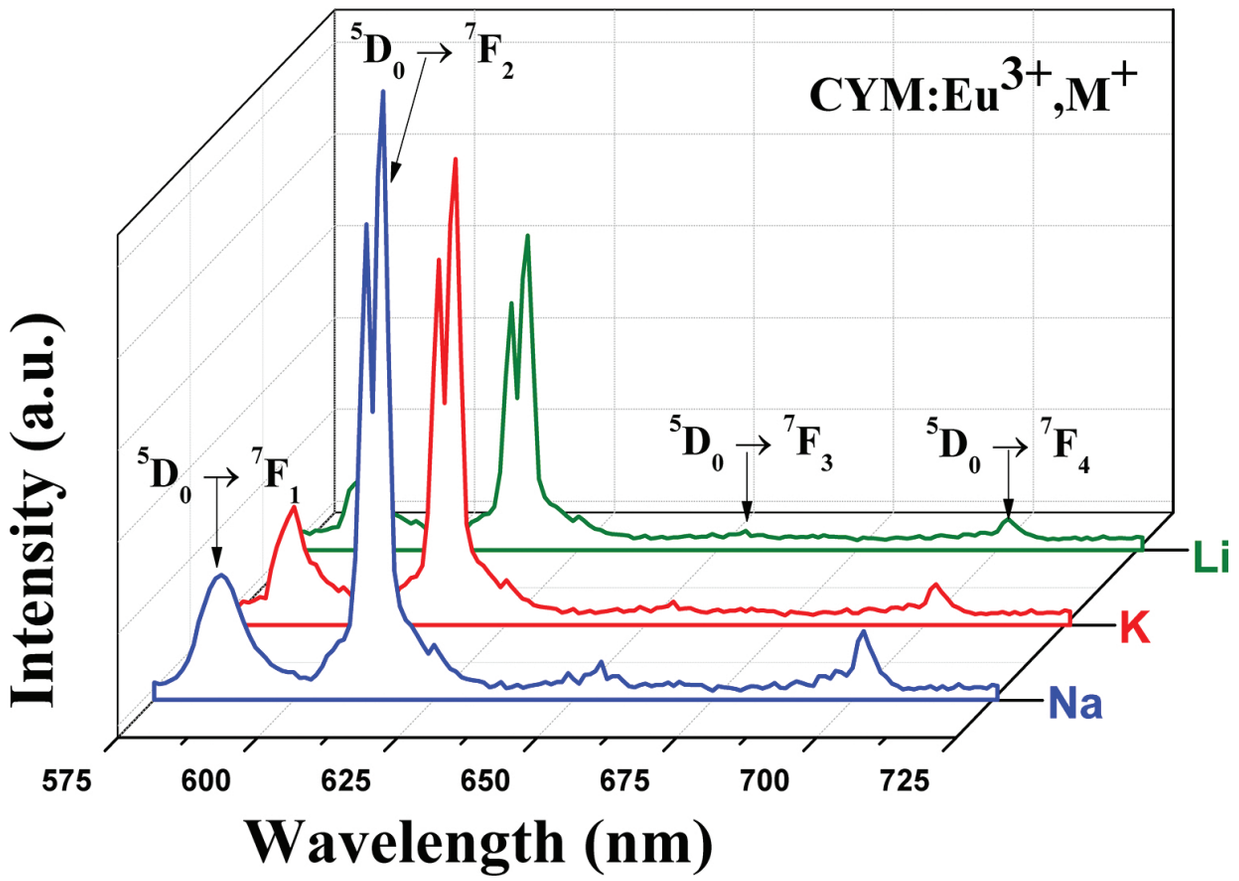

Figure 6. PL emission spectrum of the thin film phosphor $Ca_{0.5}Y(MoO_4)_2{:}Eu^{3+}$ co-doped with various alkali metal ions [Li^{+}(Green), K^{+}(Red) and Na^{+}(Blue)].

http://dx.doi.org/10.5772/65006

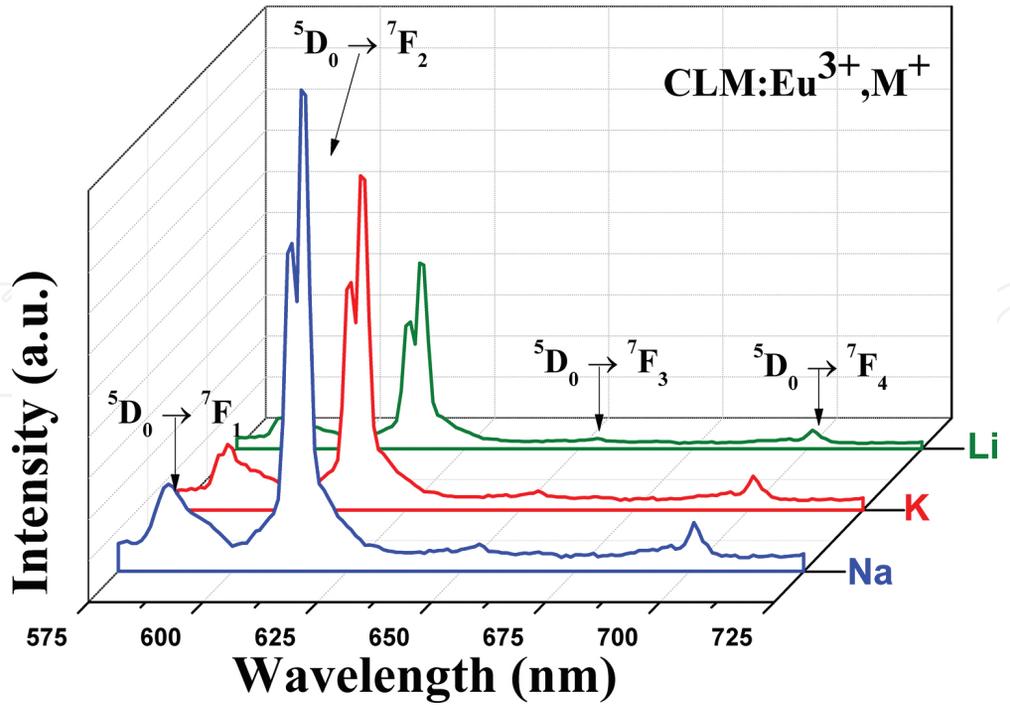

Figure 7. PL emission spectrum of the thin film phosphor $Ca_{0.5}La(MoO_4)_2:Eu^{3+}$ co-doped with various alkali metal ions [Li^+(Green), K^+(Red) and Na^+(Blue)].

3.2.2. Photoluminescence excitation studies

3.2.2.1. $Ca_{0.5}Y_{1-x}(MoO_4)_2:xLn^{3+},Na^+$ (Ln = Eu, Tb and Dy)

Figure 8a shows the room temperature PL excitation spectra of $Ca_{0.5}Y_{1-x}(MoO_4)_2:xLn^{3+}$ (Ln = Eu, Tb and Dy) thin film phosphors. The PL excitation spectrum of $Ca_{0.5}Y_{1-x}(MoO_4)_2:xEu^{3+},Na^+$ is having a wavelength range of 225–575 nm. It is showing two regions with a broad band and intense sharp peaks. The broad band is located from 225 to 350 nm with a centre at ~306 nm attributed to the O^{2-} to Eu^{3+} charge transfer band (CTB) and also designated as ligand-to-Eu^{3+} metal charge transfer transitions (LMCT) [23, 24]. Above 350 nm, intense sharp peaks are found at 362 nm ($^7F_0 \rightarrow {}^5D_4$), 382 nm ($^7F_0 \rightarrow {}^5L_7$), 395 nm ($^7F_0 \rightarrow {}^5L_6$), 416 nm ($^7F_0 \rightarrow {}^5D_3$), 465 nm ($^7F_0 \rightarrow {}^5D_2$) and 536 nm ($^7F_0 \rightarrow {}^5D_1$). Among which, the strong and intense peak is found at 395 nm. The characteristic configurations were attributed to the transition from the $^7F_0$ ground state of Eu^{3+} to the upper excited states ($^5D_{1,2,3,4}$ and $L_{6,7}$). This strongest peak in UV region is more suitable for exciting Eu^{3+} ions.

Figure 8b depicts the room temperature excitation spectrum of $Ca_{0.5}Y_{1-x}(MoO_4)_2:xTb^{3+},Na^+$ with a wavelength range of 270–390 nm in the UV region. It consists of two regions. One is from 270 to 360 nm, a highly intense and wide band designated as charge transfer band (CTB) having centred at ~295 nm is ascribed to the charge transfer of molybdate host lattice [17]. The other is due to f-f transitions of Tb^{3+} and its peak is at 376 nm ($^7F_6 \rightarrow {}^5G_6$) which is less intense than CTB. The energy transfer is being occurred from $4f^8$ to $4f^75d$ configuration of Tb^{3+} ions [17].

The excitation spectrum for the $Ca_{0.5}Y_{1-x}(MoO_4)_2$:xDy^{3+},Na^+ thin film phosphor is shown in **Figure 8c**. The wavelength of the excitation spectrum ranges from 240 to 480 nm. The strong broad band is ranging from 240 to 340 nm bears a centre at ~270 nm. Above 340 nm, the numerous intense f-f transitions of Dy^{3+} ions are found. The f-f transitions are located at 353 nm ($^6H_{15/2} \rightarrow {}^6P_{7/2}$), 367 nm ($^6H_{15/2} \rightarrow {}^6P_{5/2}$), 388 nm ($^6H_{15/2} \rightarrow {}^4I_{3/2}$), 425 nm ($^6H_{15/2} \rightarrow {}^4G_{11/2}$), 453 nm ($^6H_{15/2} \rightarrow {}^4I_{15/2}$) and 475 nm ($^6H_{15/2} \rightarrow {}^4F_{9/2}$) [25]. The highly intense peak is found at 353 nm which is the best candidate for exciting Dy^{3+} ions.

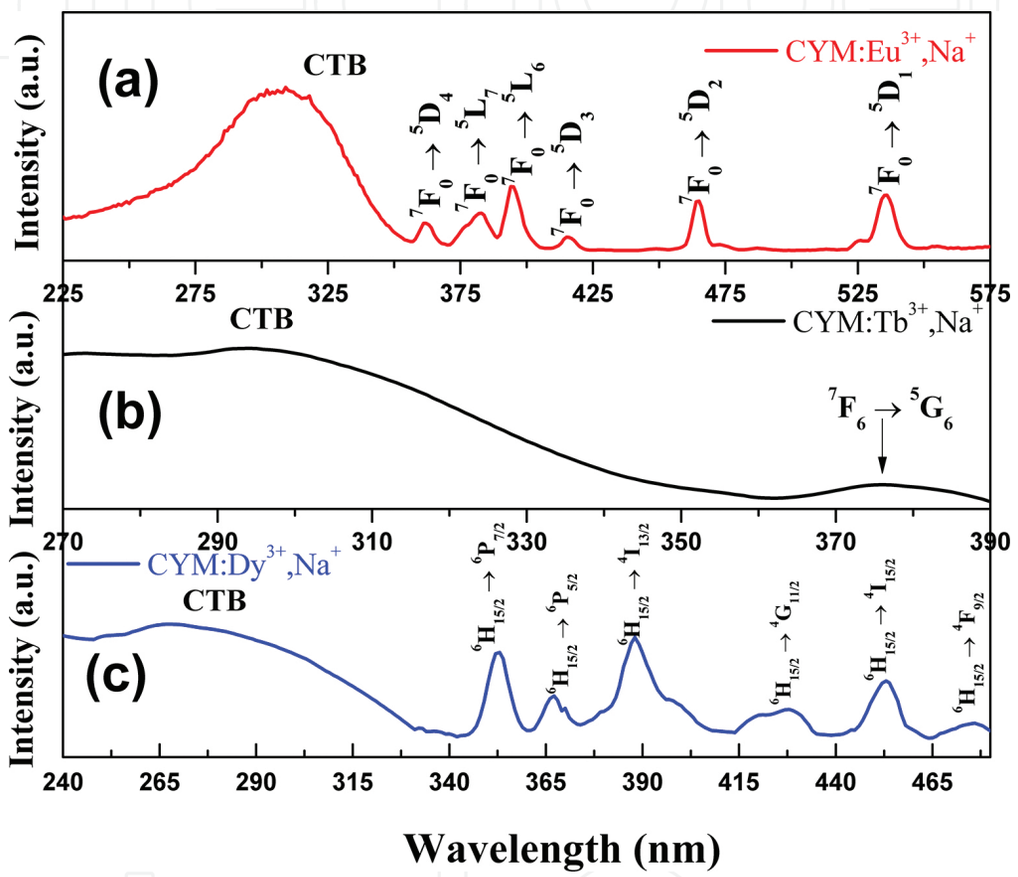

Figure 8. PL excitation spectrum (a, b, and c) for the thin film phosphors $Ca_{0.5}Y(MoO_4)_2$:Ln3+ (Ln = Eu, Tb and Dy).

3.2.2.2. $Ca_{0.5}La_{1-x}(MoO_4)_2$:$xLn^{3+}$,$Na^+$ (Ln = Eu, Tb and Dy)

The room temperature PL excitation spectra of $Ca_{0.5}La_{1-x}(MoO_4)_2$:$xLn^{3+}$ (Ln = Eu, Tb and Dy) thin phosphor films are illustrated in **Figure 9a**. The PL excitation spectrum of $Ca_{0.5}Y_{1-x}(MoO_4)_2$:xEu^{3+},Na^+ comprises of wavelength range of 200–550 nm. It consists of two regions with a wide band and highly intense sharp peaks. The wide band is found from 220 to 350 nm with a centre at ~278 nm ascribed to the O^{2-} to Eu^{3+} ligand-to-Eu^{3+} metal charge transfer transitions (LMCT) [19]. Above 350 nm, intense sharp peaks are found at 360 nm ($^7F_0 \rightarrow {}^5D_4$), 382 nm ($^7F_0 \rightarrow {}^5L_7$), 394 nm ($^7F_0 \rightarrow {}^5L_6$), 415 nm ($^7F_0 \rightarrow {}^5D_3$), 464 nm ($^7F_0 \rightarrow {}^5D_2$) and 535 nm ($^7F_0 \rightarrow {}^5D_1$). In that, the strongest and highly intense peak is found at 394 nm. This strongest peak in UV region is good for exciting Eu^{3+} ions.

http://dx.doi.org/10.5772/65006

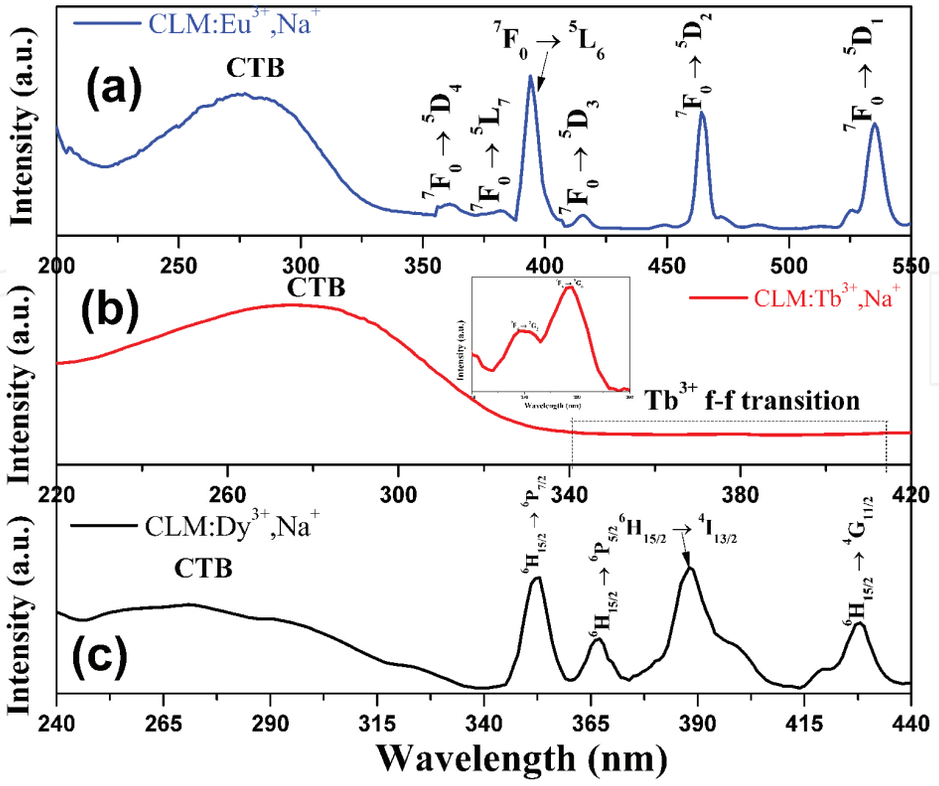

Figure 9. PL excitation spectrum (a, b, and c) for the thin film phosphors $Ca_{0.5}La(MoO_4)_2$:Ln^{3+} (Ln = Eu, Tb and Dy).

Figure 9b shows that the photoluminescence excitation spectrum of $Ca_{0.5}La_{1-x}(MoO_4)_2$:$xTb^{3+}$,$Na^+$ possess a wavelength range of 220–420 nm in the UV region. Among the two regions, the broad region is from 220 to 340 nm, ascribed to charge transfer band (CTB) which is centred at ~278 nm. The other sharp peaks are due to f-f transitions of Tb^{3+} with peaks at 369 nm ($^7F_6 \rightarrow {}^5G_5$) and 378 nm ($^7F_6 \rightarrow {}^5G_6$) is having lesser intensity than charge transfer band (CTB) [19].

The room temperature excitation spectrum for the $Ca_{0.5}La_{1-x}(MoO_4)_2$:$xDy^{3+}$,$Na^+$ thin film phosphor is depicted in **Figure 9c**. The range of the excitation spectrum is from 240 to 440 nm. The broad band ranges from 240 to 340 nm bears a centre at ~271 nm. After 340 nm, a number of highly intense f-f transitions of Dy^{3+} ions are located. The f-f transitions are found at 352 nm ($^6H_{15/2} \rightarrow {}^6P_{7/2}$), 367 nm ($^6H_{15/2} \rightarrow {}^6P_{5/2}$), 388 nm ($^6H_{15/2} \rightarrow {}^4I_{3/2}$) and 428 nm ($^6H_{15/2} \rightarrow {}^4G_{11/2}$) [19]. The most intense peak that is situated at ~352 nm is fit for exciting Dy^{3+} ions.

3.2.3. Photoluminescence emission studies

3.2.3.1. $Ca_{0.5}Y_{1-x}(MoO_4)_2$:xLn^{3+},Na^+ (Ln = Eu, Tb and Dy)

The room temperature PL emission spectra for $Ca_{0.5}Y_{1-x}(MoO_4)_2$:xLn^{3+},Na^+ (Ln = Eu, Tb and Dy) thin phosphor films are shown in **Figure 10a**. The emission spectra monitored at 395 nm UV excitation for $Ca_{0.5}Y_{1-x}(MoO_4)_2$:xEu^{3+},Na^+ illustrates a number of intra-configurational 4f-4f transitions arising from Eu^{3+} $^5D_0$ excited state to the ^7F_J (J = 1, 2, 3 and 4) ground states [26–28]. Upon other excitations and also with LMCT, there is no significant change in emission spectra.

The strong and most intense emission peak is found at 616 nm upon 395 nm UV excitation is ascribed to the $^5D_0 \rightarrow {}^7F_2$ electric-dipole transition depicts hypersensitive red emission which is parity forbidden ($\Delta J = 2$) [26]. Also, it shows two sub-peaks arises due to Stark energy splitting, that is (2J + 1) Stark components of J-degeneracy splitting [27]. The predominant electric-dipole transition signifies that Eu^{3+} ions are found at sites without inversion symmetry. The other transitions found at 587 nm ($^5D_0 \rightarrow {}^7F_1$) show orange emission owing to magnetic-dipole transition. The other relatively weaker transitions are located at 655 nm ($^5D_0 \rightarrow {}^7F_3$) and 702 nm ($^5D_0 \rightarrow {}^7F_4$) [28]. The red emission to orange emission (R/O) ratio for the thin film phosphor is 5.2536. From these findings, it is evident that $Ca_{0.5}Y_{1-x}(MoO_4)_2{:}xEu^{3+},Na^+$ possess scheelite tetragonal structure having C_{3v} site symmetry could be used for display applications.

The PL emission spectrum for $Ca_{0.5}Y_{1-x}(MoO_4)_2{:}xTb^{3+},Na^+$ upon ~295 nm UV excitation is shown in **Figure 10b**, comprises four PL emission bands having peaks at 489 nm ($^5D_4 \rightarrow {}^7F_6$), 545 nm ($^5D_4 \rightarrow {}^7F_5$), 587 nm ($^5D_4 \rightarrow {}^7F_4$) and 621 nm ($^5D_4 \rightarrow {}^7F_3$). In these emission peaks, the highly remarkable green colour is located at 545 nm related to the predominant transition $^5D_4 \rightarrow {}^7F_5$ [27]. It is due to the energy transfer from the host which is populating only $^5D_4$ level. The dominant emission peak which is having two sub peaks is due to the Stark energy splitting and forms the suitable candidate for display applications.

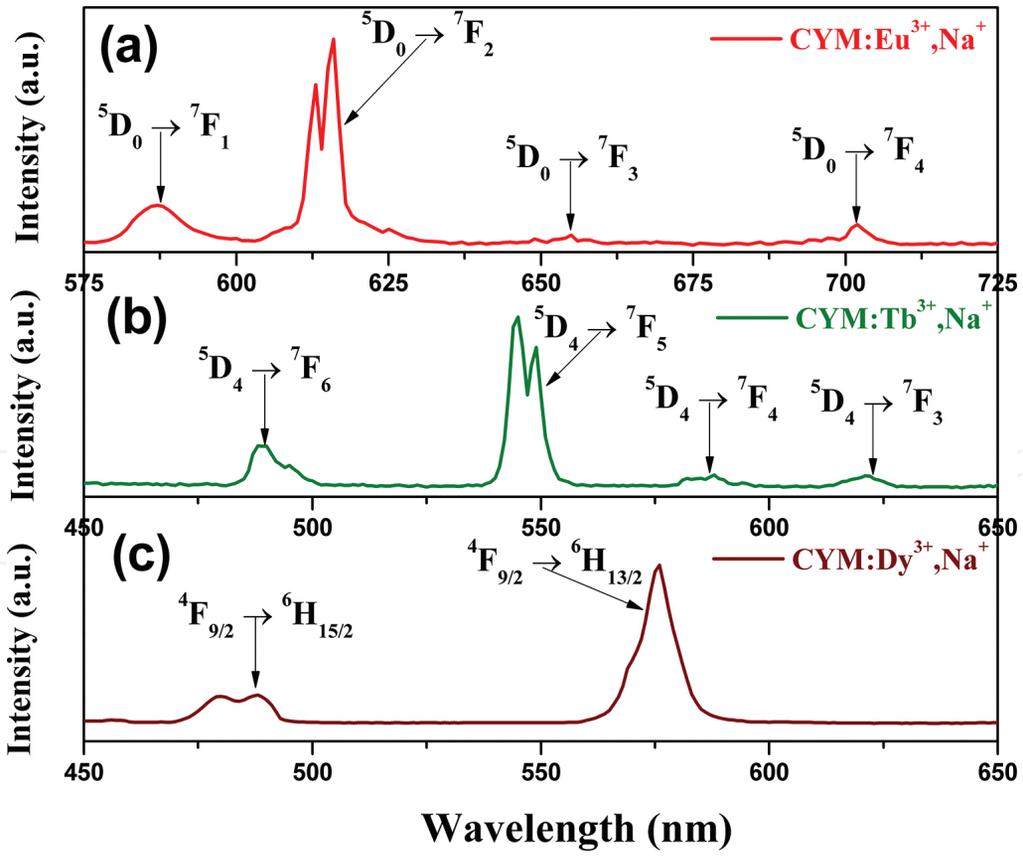

Figure 10. PL emission spectra (a, b, and c) of the thin film phosphors $Ca_{0.5}Y(MoO_4)_2{:}Ln^{3+},M^+$ (Ln = Eu, Tb and Dy; M = Na).

http://dx.doi.org/10.5772/65006

The room temperature PL emission spectrum (**Figure 10c**) for the thin film phosphor $Ca_{0.5}Y_{1-x}(MoO_4)_2$:xDy^{3+},Na^+ excited upon 353 nm excitation wavelength. The emission spectrum consists of two major peaks with respective peaks at 485 nm ascribed to magnetic dipole transition of ($^4F_{9/2} \rightarrow {}^6H_{15/2}$) and 576 nm related to forced electric dipole transition of $^4F_{9/2} \rightarrow {}^6H_{13/2}$. The magnetic dipole transition is lesser sensitive to the coordination environment [27, 28]. The forced electric dipole transition is appeared only in the case of Dy^{3+} ions which are found at the local sites without inversion centre symmetry [28]. The respective blue emission having a centre at 485 nm is relatively lower intense than predominant yellow emission. The yellow-to-blue line ratio is 6.8026 which signifies that forced electric dipole transition is in dominance thereby indicating that the Dy^{3+} ions would found at the local sites with non-inversion centre symmetry in the $Ca_{0.5}Y_{1-x}(MoO_4)_2$ host.

3.2.3.2. $Ca_{0.5}La_{1-x}(MoO_4)_2$:$xLn^{3+}$,$Na^+$ (Ln = Eu, Tb and Dy)

The room temperature PL excitation spectrum of $Ca_{0.5}La_{1-x}(MoO_4)_2$:$xEu^{3+}$ thin phosphor films monitored at 394 nm excitation wavelength is shown in **Figure 11a**, consists of numerous intra-configurational 4f-4f transitions. As the Eu^{3+} concentration in the $Ca_{0.5}La(MoO_4)_2$ host lattices increases, the photoluminescence emission of the host is suppressed due to the overcoming of Eu^{3+} ions. The intensities of the different $^5D_0 \rightarrow {}^7F_J$ transitions might depend on the local symmetry of crystal field of Eu^{3+} ions [19]. The highly intense and strong emission peak is located at 615 nm upon 394 nm UV excitation corresponds to the $^5D_0 \rightarrow {}^7F_2$ electric-dipole transition showing hypersensitive red emission with parity forbidden ($\Delta J = 2$). The split-up in the peaks is due to the Stark energy splitting, which is having (2J + 1) Stark components of J-degeneracy splitting [28]. The predominant electric-dipole transition implies that Eu^{3+} ions would be situated at sites with non-inversion symmetry [15]. The transitions located at 586 nm show emission in the orange region which is associated with magnetic-dipole transition ($^5D_0 \rightarrow {}^7F_1$) and is not affected by the chemical surroundings of Eu^{3+}. The remaining transitions at 654 nm ($^5D_0 \rightarrow {}^7F_3$) and 701 nm ($^5D_0 \rightarrow {}^7F_4$) are the weakest ones. The red-to-orange emission (R/O) ratio of the phosphor is 5.5311 which suggests the sites symmetry of the respective Eu^{3+} ions. Based on these observations, it is suggested that $Ca_{0.5}La_{1-x}(MoO_4)_2$:$xEu^{3+}$,$Na^+$ might be a suitable phosphor candidate for solid-state lighting applications.

The PL emission spectrum for $Ca_{0.5}La_{1-x}(MoO_4)_2$:$xTb^{3+}$,$Na^+$ recorded at ~278 nm UV excitation is shown in **Figure 11b** which consists of four PL emission peaks at 489 nm ($^5D_4 \rightarrow {}^7F_6$), 545 nm ($^5D_4 \rightarrow {}^7F_5$), 585 nm ($^5D_4 \rightarrow {}^7F_4$) and 621 nm ($^5D_4 \rightarrow {}^7F_3$). Among these emission peaks, the sensitive green colour is located at 545 nm associated to the predominant transition $^5D_4 \rightarrow {}^7F_5$ [19]. It is based on the energy transfer from the host populates only $^5D_4$ level. The dominant emission peak possesses two sub peaks which correspond to the Stark energy splitting.

The room temperature PL emission spectrum (**Figure 11c**) for the thin phosphor film $Ca_{0.5}La_{1-x}(MoO_4)_2$:$xDy^{3+}$,$Na^+$ excited with 352 nm excitation wavelength. The emission spectrum comprises of two major peaks with peak positions at 477 nm attributed to magnetic dipole transition of ($^4F_{9/2} \rightarrow {}^6H_{15/2}$) and 570 nm corresponds to forced electric dipole transition of $^4F_{9/2} \rightarrow {}^6H_{13/2}$ [25]. The magnetic dipole transition is least sensitive to the coordination environment. The forced electric dipole transition would be found only in the case of Dy^{3+} ions situated at

the local sites without inversion symmetry [19]. The emission in the blue region having a centre at 477 nm is having relatively least intense than predominant yellow emission. The yellow-to-blue line ratio is 6.0076 which implies that the forced electric dipole transition is most dominant hence indicating that the Dy^{3+} ions are situated at the local sites with non-inversion symmetry in the $Ca_{0.5}La_{1-x}(MoO_4)_2$ host.

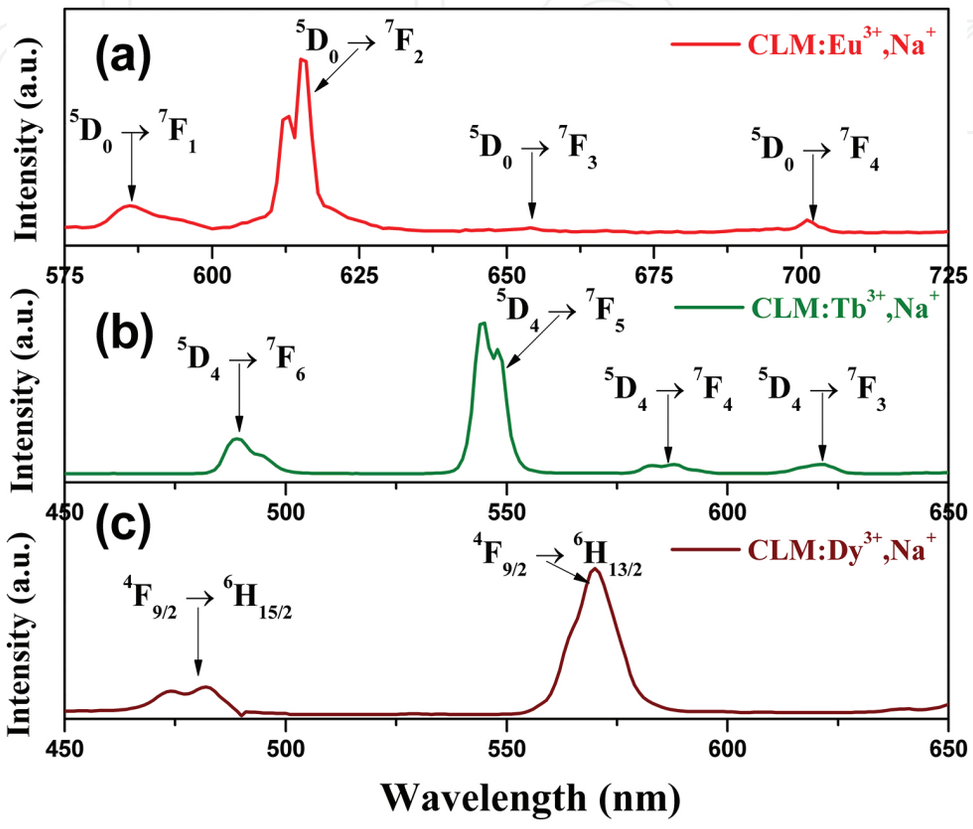

Figure 11. PL emission spectra (a, b, and c) of the thin film phosphors $Ca_{0.5}La(MoO_4)_2:Ln^{3+},M^+$ (Ln = Eu, Tb and Dy; M = Na).

3.3. Photometric characterization and decay-time analysis

Figures 12a, **b** and **13a**, **b** show the decay time profile and Commission Internationale de I'Eclairage (CIE) colour chromaticity coordinates of the $Ca_{0.5}Y_{1-x}(MoO_4)_2:xLn^{3+},Na^+$ (Ln = Eu, Tb and Dy) and $Ca_{0.5}La_{1-x}(MoO_4)_2:xLn^{3+},Na^+$ (Ln = Eu, Tb and Dy) phosphors. The CIE colour chromaticity coordinate of these phosphors was estimated and is given in **Table 1**. Furthermore, to know about the characteristic emission of these phosphors, the value of colour purity was derived by the equation [24]

$$\text{Colourpurity} = \frac{\sqrt{(x-x_i)^2+(y-y_i)^2}}{\sqrt{(x_d-x_i)^2+(y_d-y_i)^2}}100 \tag{1}$$

http://dx.doi.org/10.5772/65006

where (x, y) is denoted as CIE chromaticity coordinate of the synthesized sample, (x_i, y_i) is the CIE white illumination, and (x_d, y_d) is the CIE chromaticity coordinate of the dominant wavelength. Thus, the colour purities of the $Ca_{0.5}Y_{1-x}(MoO_4)_2:xEu^{3+},Na^+$, $Ca_{0.5}Y_{1-x}(MoO_4)_2:xTb^{3+},Na^+$ and $Ca_{0.5}Y_{1-x}(MoO_4)_2:xDy^{3+},Na^+$ phosphors are 90.0, 87.5 and 81.3%, respectively. Similarly, the colour purities of the $Ca_{0.5}La_{1-x}(MoO_4)_2:xEu^{3+},Na^+$ $Ca_{0.5}La_{1-x}(MoO_4)_2:xTb^{3+},Na^+$ and $Ca_{0.5}La_{1-x}(MoO_4)_2:xDy^{3+},Na^+$ phosphors are 95.0, 91.9 and 81.7%. From the results, it is suggested that these phosphors with remarkable CIE chromaticity coordinate with high colour purities might be suitable for applications in display devices as the best red, green and yellow emitting phosphors.

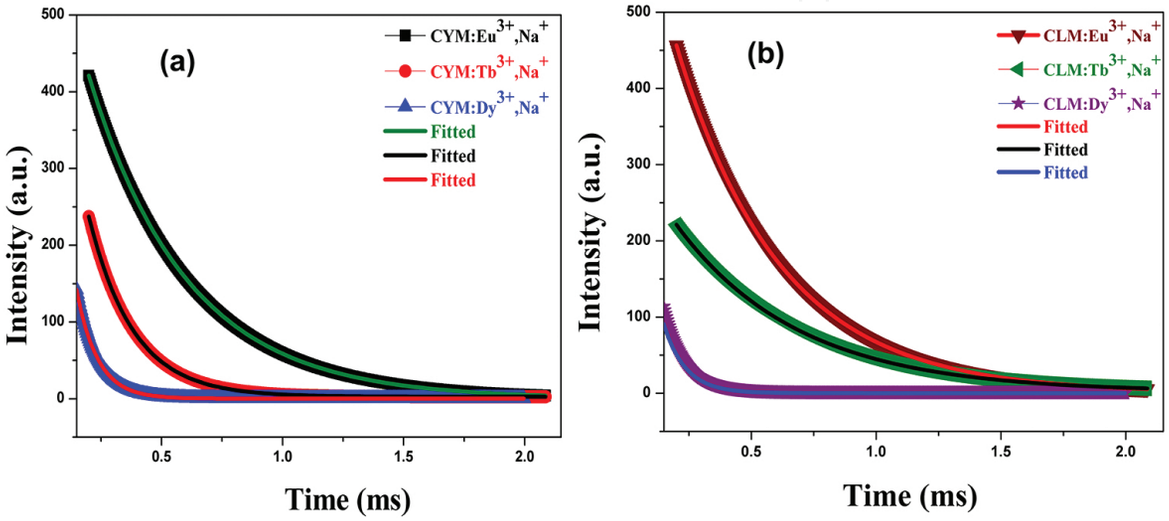

Figure 12. Luminescence decay profiles (a and b) for the thin film phosphors $Ca_{0.5}R_{1-x}(MoO_4)_2:xLn^{3+}$ (R^{3+} = Y, La),Na^+ (Ln = Eu, Tb and Dy).

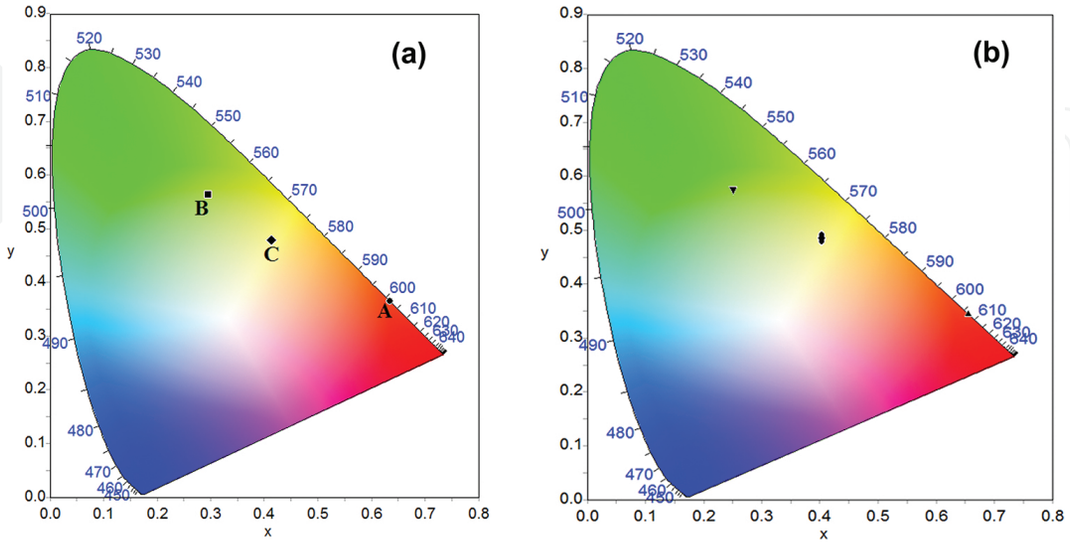

Figure 13. CIE diagram (a, b) for the thin film phosphors $Ca_{0.5}Y(MoO_4)_2:Ln^{3+},Na^+$ (Ln = (A) Eu, (B) Tb and (C) Dy).

The representative PL decay curves for luminescence emission for the phosphors $Ca_{0.5}Y_{1-x}(MoO_4)_2{:}xLn^{3+},Na^+$ (Ln = Eu, Tb and Dy) and $Ca_{0.5}La_{1-x}(MoO_4)_2{:}xLn^{3+},Na^+$ (Ln = Eu, Tb and Dy) are shown in **Figure 12a**, **b**. This can be fitted well into a single exponential function [15, 27] as

$$I = I_0 \exp\left(\frac{-t}{\tau}\right) \tag{2}$$

where I_0 is the luminescence intensity at times $t = 0$ and τ is its associated luminescence lifetime. The photometric quantities and luminescence decay time values are given in **Table 1**.

Phosphor	CCT (K)	CRI	Colour coordinates		LER (lm W^{-1})	Colour purity (%)	τ (ms)
			x	*y*			
$Ca_{0.5}Y(MoO_4)_2{:}Eu^{3+},Na^+$	1149	33	0.635	0.365	162	90.0	0.462
$Ca_{0.5}Y(MoO_4)_2{:}Tb^{3+},Na^+$	N/A	26	0.296	0.564	491	87.5	0.455
$Ca_{0.5}Y(MoO_4)_2{:}Dy^{3+},Na^+$	3658	18	0.414	0.478	525	81.3	0.172
$Ca_{0.5}La(MoO_4)_2{:}Eu^{3+},Na^+$	1196	42	0.656	0.343	321	95.0	0.481
$Ca_{0.5}La(MoO_4)_2{:}Tb^{3+},Na^+$	6850	12	0.251	0.570	530	91.9	0.485
$Ca_{0.5}La(MoO_4)_2{:}Dy^{3+},Na^+$	4195	16	0.404	0.485	462	81.7	0.187

Table 1. Photometric parameters, color purity and luminescence decay time for the phosphors $Ca_{0.5}R_{1-x}(MoO_4)_2{:}xLn^{3+}$, Na^+ (R = Y, La; Ln = Eu, Tb and Dy).

3.4. Photoluminescence emission studies from nano-architectures

The thin phosphor films grown from nano-powder are being synthesized by the hydrothermal method, and the synthesis procedure is described previously by our group [17]. The luminescence emission intensity is being enhanced by co-doping of alkali metal ions. Furthermore, for the co-doping of alkali precursors, instead of using alkali chloride, alkali carbonates were taken and converted them into alkali nitrates. These alkali nitrates were co-doped with the existing precursors following the hydrothermal method nano-powders were synthesized and thin films were deposited from these powders [17]. The room temperature PL emission spectrum for $Ca_{0.5}R_{1-x}(MoO_4)_2{:}xEu^{3+},Na^+$ (R = Y, La) as the representative thin phosphor films are shown in **Figure 14**. The emission spectra monitored at 395 nm UV excitation for both the phosphors shows a number of intra-configurational f-f transitions. The strong and most intense emission peak is found at 616 nm for $Ca_{0.5}Y_{1-x}(MoO_4)_2{:}xEu^{3+},Na^+$ and 615 nm for $Ca_{0.5}La_{1-x}(MoO_4)_2{:}xEu^{3+},Na^+$ is attributed to the $^5D_0 \rightarrow {}^7F_2$ electric-dipole transition possess hypersensitive red emission [15, 28, 29]. The Stark energy splitting is mildly shown for both the phosphors. It is noticed that the splitting of the electric dipole transition is uniform and homogeneous between the two thin phosphor films. The intensity of the spectral peaks for the nano-thin phosphor film is nearly close

http://dx.doi.org/10.5772/65006

to that of those from the bulk thin phosphor film, as peak intensity is related to reduced particle size and improved homogeneity [17, 29]. The dominant electric-dipole transition suggests that Eu^{3+} ions are found at sites with non-inversion symmetry [30]. The other transitions found at 587 nm ($^5D_0 \rightarrow {}^7F_1$) for $Ca_{0.5}Y_{1-x}(MoO_4)_2:xEu^{3+},Na^+$ and 586 nm ($^5D_0 \rightarrow {}^7F_1$) for $Ca_{0.5}La_{1-x}(MoO_4)_2:xEu^{3+},Na^+$ show orange emission due to magnetic-dipole transition. The other relatively weaker transitions are found at 654 nm ($^5D_0 \rightarrow {}^7F_3$) and 702 nm ($^5D_0 \rightarrow {}^7F_4$) for both the nano-thin phosphor films. The photometric parameters for both the phosphors are under further investigation. From these results, it is indicated that $Ca_{0.5}R_{1-x}(MoO_4)_2:xEu^{3+},Na^+$ (R = Y, La) phosphors are best candidates for display applications.

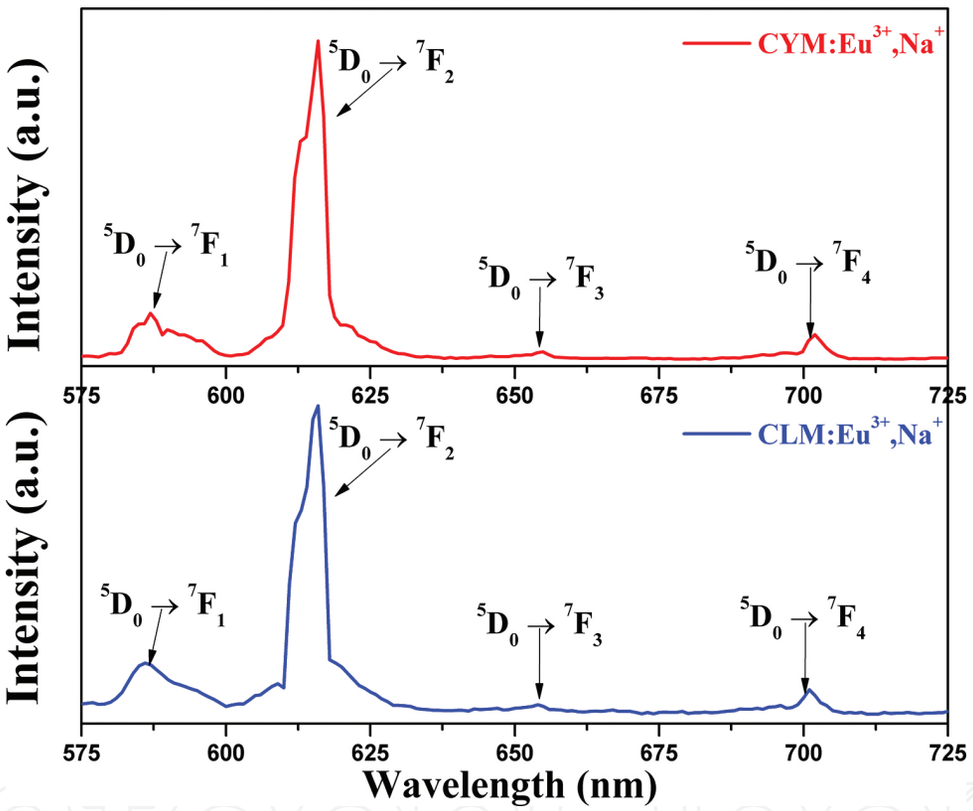

Figure 14. PL emission spectrum of the thin film phosphors $Ca_{0.5}Y(MoO_4)_2:Eu^{3+},Na^+$ and $Ca_{0.5}La(MoO_4)_2:Eu^{3+},Na^+$ prepared from nano-phosphors.

4. Conclusion

In conclusion, the nano-sized single crystalline $Ca_{0.5}La_{1-x}(MoO_4)_2:xEu^{3+},M^+$ ceramic thin phosphor films deposited on quartz substrates by pulsed laser deposition technique using Nd-YAG laser source in an ultra-high vacuum (UHV). The FESEM images exhibited the spherical-shaped phosphor particles. XRD patterns revealed the scheelite-type crystal structure without any impurity phases. By using AFM, the surface topographies and distributions of grains were

investigated. Upon optical excitation, Eu-, Tb, and Dy-doped $Ca_{0.5}La_{1-x}(MoO_4)_2$:$x$$Eu^{3+}$,$M^+$ thin phosphor films showed characteristic emissions in the bright-red, green and yellow regions, respectively. The obtained results suggested that the deposited thin film phosphors could serve as efficient materials for electroluminescence and display applications.

Conflict of interest

The authors declare that there is no conflict of interests regarding the publication of this chapter.

Acknowledgements

Work incorporated in this chapter was supported by Science and Engineering Research Board (SERB), (SR/FTP/PS-135/2011) Govt. of India. The authors apologize for inadvertent omission of any pertinent references.

Author details

Jagannathan Thirumalai[1*], Venkatakrishnan Mahalingam[1] and Rajagopalan Krishnan[2]

*Address all correspondence to: thirumalaijg@gmail.com; jthirumalai@bsauniv.ac.in

1 Department of Physics, School of Physical and Chemical Sciences, B. S. Abdur Rahman University, Vandalur, Chennai, Tamil Nadu, India

2 Department of Physics, Rajalakshmi Institute of Technology, Kuthambakkam, Chennai, Tamil Nadu, India

References

[1] Park S W, Moon B K, Choi B C, Jeong J H, Bae J S, Kim K H: Red photoluminescence of pulsed laser deposited Eu:$NaY(MoO_4)_2$ thin film phosphors on sapphire substrates. Curr. Appl. Phys. 2012;12:S150–S155. doi:10.1016/j.cap.2012.02.048

[2] Krishnan R, Thirumalai J: Synthesis and up/down conversion luminescence properties of $Na_{0.5}R_{0.5}MoO_4$:Ln^{3+} (R^{3+} = La, Gd), (Ln^{3+} = Eu, Tb, Dy, Yb/Er) thin phosphor films grown by pulsed laser deposition technique. RSC Adv. 2014;4:64258–64266. doi:10.1039/c4ra11274a

[3] Mahalingam V, Thirumalai J, Krishnan R, Mantha S: Up/down conversion luminescence and charge compensation investigation of $Ca_{0.5}Y_{1-x}(WO_4)_2:xLn^{3+}$ (Ln = Pr, Sm, Eu, Tb, Dy, Yb/Er) phosphors. Spectrochim. Acta A. 2016;152:172–180. doi:10.1016/j.saa.2015.06.129

[4] Barreca D, Depero L E, Noto V D, Rizzi G A, Sangaletti L, Tondello E: Thin films of bismuth vanadates with modifiable conduction properties. Chem. Mater. 1999;11:255–261. doi:10.1021/cm980725q

[5] Yanagihara M, Yusop M Z, Tanemura M, Ono S, Nagami T, Fukuda K, Suyama T, Yokota Y, Yanagida T, Yoshikawa A: Vacuum ultraviolet field emission lamp utilizing $KMgF_3$ thin film phosphor. APL Mater. 2014;2:046110(1–6). doi:10.1063/1.4871915

[6] Shaikh P A, Thakare V P, Late D J, Ogale S: A back-to-back MOS-Schottky (Pt-SiO_2-Si-C-Pt) nano-heterojunction device as an efficient self-powered photodetector: one step fabrication by pulsed laser deposition. Nanoscale. 2014;6:3550–3556. doi:10.1039/C3NR06525A

[7] Patel P K, Yadav K L, Kaur G: Reduced dielectric loss in $Ba_{0.95}Sr_{0.05}(Fe_{0.5}Nb_{0.5})O_3$ thin film grown by pulsed laser deposition. RSC Adv. 2014;4:28056–28061. doi:10.1039/C4RA03502J

[8] Lin C C, Liu R S: Advances in phosphors for light-emitting diodes. J. Phys. Chem. Lett. 2011;11:1268–1277. doi:10.1021/jz2002452

[9] Li Y Q, van Steen J E J, van Krevel J W H, Botty G, Delsing A C A, Disalvo F J, de With G, Hintzen H T: Luminescence properties of red-emitting $M_2Si_5N_8:Eu^{2+}$(M = Ca, Sr, Ba) LED conversion phosphors. J. Alloys Compd. 2006;417:273–279. doi:10.1016/j.jallcom.2005.09.041

[10] Aboulaich A, Michalska M, Schneider R, Potdevin A, Deschamps J, Deloncle R, Chadeyron G, Mahiou R: Ce-doped YAG nanophosphor and red emitting $CuInS_2$/ZnS core/shell quantum dots for warm white light-emitting diode with high color rendering index. Appl. Mater. Interfaces. 2014;6:252–258. doi:10.1021/am404108n

[11] Zhang L, Lu Z, Han P, Wang L, Zhang Q: Synthesis and photoluminescence of Eu^{3+}-activated double perovskite NaGdMg(W, Mo)O_6—a potential red phosphor for solid state lighting. J. Mater. Chem. C. 2013;1:54–57. doi:10.1039/C2TC00189F

[12] Li K, Geng D, Shang M, Zhang Y, Lian H, Lin J: Color-tunable luminescence and energy transfer properties of $Ca_9Mg(PO_4)_6F_2:Eu^{2+},Mn^{2+}$ phosphors for UV-LEDs. J. Phys. Chem. C. 2014;118:11026–11034. doi:10.1021/jp501949m

[13] Yang H, Wang W, Liu Z, Li G: Homogeneous epitaxial growth of AlN single-crystalline films on 2 inch-diameter Si (1 1 1) substrates by pulsed laser deposition. Cryst. Eng. Comm. 2013;15:7171–7176. doi:10.1039/C3CE40886H

[14] Atanasov P A, Tomov R I, Perriere J, Eason R W, Vainos N, Klini A, Zherikhin A, Millon E: Growth of Nd: potassium gadolinium tungstate thin-film waveguides by pulsed laser deposition. Appl. Phys. Lett. 2000;76:2490–2492. doi:10.1063/1.126385

[15] Mahalingam V, Thirumalai J, Krishnan R, Chandramohan R: Potential visible light emitting rare-earth activated $Ca_{0.5}Y_{1-x}(MoO_4)_2$:$x$$RE^{3+}$ (RE = Pr, Sm, Eu, Tb, Dy) phosphors for solid state lighting applications. J. Mater. Sci. Mater. Electron. 2015;26:842–852. doi: 10.1007/s10854-014-2473-2

[16] Eason R, editor. Pulsed laser deposition of thin films: Applications–led growth of functional materials. John Wiley & Sons, Inc., Hoboken, New Jersey : Wiley; 2007 p. 1–682. DOI: 10.1002/0470052120

[17] Xia Z, Chen D: Synthesis and luminescence properties of $BaMoO_4$:Sm^{3+} phosphors. J. Am. Ceram. Soc. 2010;93:1397–1401. doi:10.1111/j.1551-2916.2009.03574.x

[18] Krishnan R, Thirumalai J, Mahalingam V, Mantha S, Lavanya M: Synthesis, luminescence and photometric characteristics of $Ca_{0.5}La(MoO_4)_2$:Ln^{3+} (Ln = Eu, Tb, Dy) phosphors. Mater. Chem. Phys. 2015;162:41–49. doi:10.1016/j.matchemphys.2015.04.050

[19] Du P, Yu J S: Dual-enhancement of photoluminescence and cathodoluminescence in Eu^{3+}-activated $SrMoO_4$ phosphors by Na^+ doping. RSC Adv. 2015;5:60121–60127. doi: 10.1039/c5ra06053b

[20] Liu X, Li L, Noh H M, Jeong J H, Jang K, Shin D S: Controllable synthesis of uniform $CaMoO_4$:Eu^{3+},M^+ (M = Li, Na, K) microspheres and optimum luminescence properties. RSC Adv. 2015;5:9441–9454. doi:10.1039/c4ra12183j

[21] Luitel H N, Chand R, Watari T: $CaMoO_4$:RE^{3+},Yb^{3+},M^+ phosphor with controlled morphology and color tunable upconversion. Displays. 2016;42:1–8. doi:10.1016/j.displa.2015.12.004

[22] Blasse G, Grabmaier B C, editors. Luminescent materials. Berlin: Springer; 1994.

[23] Som S, Das S, Dutta S, Visser H G, Pandey M K, Kumar P, Dubey R K, Sharma S K: Synthesis of strong red emitting Y_2O_3:Eu^{3+} phosphor by potential chemical routes: comparative investigations on the structural evolutions, photometric properties and Judd-Ofelt analysis. RSC Adv. 2015;5:70887–70898. doi:10.1039/c5ra13247a

[24] Mahalingam V, Thirumalai J, Krishnan R, Chandramohan R: Controlled synthesis and luminescence properties of $Ca_{0.5}Y_{1-x}(MoO_4)$:$x$$RE^{3+}$ (RE = Eu, Pr, Sm, Tb, Dy, Yb/Er, Yb/Tm and Yb/Ho) phosphors by hydrothermal method versus pulsed laser deposition. Electron. Mater. Lett. 2016;12:32–47. doi:10.1007/s13391-015-5248-x

[25] Dutta S, Som S, Sharma S K: Luminescence and photometric characterization of K^+ compensated $CaMoO_4$:Dy^{3+} nanophosphors. Dalton Trans. 2013;42:9654–9661. doi: 10.1039/c3dt50780g

[26] Saraf R, Shivakumara C, Dhananjaya N, Behera S, Nagabhushana H: Photoluminescence properties of Eu^{3+} activated $CaMoO_4$ phosphors for WLEDs applications and its Judd-Ofelt analysis. J. Mater. Sci. 2015;50:287–298. doi:10.1007/s10853-014-8587-3

[27] Krishnan R, Thirumalai J, Thomas S, Gowri M: Luminescence and magnetic behaviour of almond like $(Na_{0.5}La_{0.5})MoO_4$:RE^{3+} (RE = Eu, Tb, Dy) nanostructures. J. Alloys Compd. 2014;604:20–30. doi:10.1016/j.jallcom.2014.03.065

[28] Krishnan R, Thirumalai J: Up/down conversion luminescence properties of $(Na_{0.5}Gd_{0.5})MoO:Ln^{3+}$ (Ln = Eu, Tb, Dy, Yb/Er, Yb/Tm and Yb/Ho) microstructures: synthesis, morphology, structural and magnetic investigation. New J. Chem. 2014;38:3480–3491. doi:10.1039/c4nj00165f

[29] Gupta S K, Sahu M, Ghosh P S, Tyagi D, Saxena M K, Kadam R M: Energy transfer dynamics and luminescence properties of Eu^{3+} in $CaMoO_4$ and $SrMoO_4$. Dalton Trans. 2015;44:18957–18969. doi:10.1039/c5dt03280f

[30] Singh B P, Parchur A K, Ningthoujam R S, Ansari A A, Singh P, Rai S B: Enhanced photoluminescence in $CaMoO_4$ by Gd^{3+} co-doping. Dalton Trans. 2014;43:4779–4789. doi:10.1039/c3dt53408a

IntechOpen